Causing the Effect: Driving the Unruh Phenomenon

Kevin Player[*][†]

August 10, 2025

> The Unruh effect tells us that what we call particles is really just a matter of perspective.
>
> Lee Smolin

Abstract

We present a framework that connects the thermal Unruh effect to a localized, non-thermal excitation picture. Using modular automorphisms, we track mode localization across nested Rindler wedges and construct compact wave-packet approximations via parabolic cylinder functions. This yields a smooth transition from global Rindler modes to fully localized excitations, supporting a causal, source-based interpretation in which the Unruh response arises from thrust, a directed, localized energy input, rather than passive detection of pre-existing vacuum correlations.

1 Introduction

The Unruh effect[1] states that uniformly accelerated observers perceive the Minkowski vacuum as a thermal state filled with particles. In this work, we develop a complementary viewpoint by examining how localization affects the thermal character of the field. In Section 2, we review the Unruh effect, including the relevant mode expansions and Bogoliubov transformations. In Section 3, we apply a classical source construction to inject particles into the field.

Section 4 explores partial localization by considering sub-regions of the Rindler wedge related through space-like translations and reflections, transformations that correspond to modular automorphisms in the associated operator algebras. We then use parabolic cylinder functions to construct a smooth interpolation between eternal Rindler modes and fully localized modes. Finally, in Section 5, we interpret the implications of our construction.

These results suggest a complementary interpretation: The Unruh effect arises from localized, non-thermal excitations, akin to a thrust driving the field.

2 Preliminaries

We draw notation and standard results from Frodden and Valdés [3]. Let $\hbar = c = 1$. We consider a uniformly accelerating observer in 1+1 dimensional Minkowski spacetime with

---

[*]kplayer@andrew.cmu.edu

[†]kjplaye@gmail.com

metric signature $\eta = (-1, +1)$. The extension to 1+3 dimensions does not affect the key physics of the Unruh effect, so we restrict to the (t,x) plane where the boost is occurring. We only consider free scalar fields in this note.

Consider the free scalar massless Lagrangian

$$\mathcal{L}_{free} = -\frac{1}{2}\eta^{\mu\nu}\partial_\mu\phi\partial_\nu\phi. \tag{1}$$

We consider positive frequency modes with dispersion relation $\omega_k = |k| > 0$ as solutions to the resulting Klein-Gordon equation

$$\Box\phi = -\frac{\partial^2\phi}{\partial t^2} + \frac{\partial^2\phi}{\partial x^2} = 0, \tag{2}$$

where $\Box = \eta^{\mu\nu}\partial_\mu\partial_\nu$. We expand ϕ in terms of ladder operators $a_k, a_k^\dagger$

$$\phi(x,t) = \int \mathrm{d}k\, a_k\varphi_k(x,t) + \text{h.c.} \tag{3}$$

where

$$\varphi(x,t) = \frac{1}{\sqrt{4\pi\omega_k}}e^{i(kx-\omega_k t)}. \tag{4}$$

are pure Minkowkski positive frequency waves normalized with respect to the Klein-Gordon inner product over a Cauchy surface Σ (usually $t = 0$)

$$\langle f,g\rangle_{KG} = i\int_\Sigma \mathrm{d}x(f^*\partial_t g - \partial_t f^* g). \tag{5}$$

2.1 Rindler Coordinates

To describe the physics from the point of view of a uniformly accelerating observer, we introduce Rindler coordinates [3, 4] covering a right wedge

$$W = \{(x,t) : x > |t|\} \tag{6}$$

with apex at the origin, pictured[1] in Figure 1; with coordinates

$$t = \frac{1}{a}e^{a\xi}\sinh(a\eta) \tag{7}$$

$$x = \frac{1}{a}e^{a\xi}\cosh(a\eta) \tag{8}$$

The constant acceleration parameter a is introduced explicitly to make the dependence of the Unruh temperature, $T = \frac{a}{2\pi}$, manifest in subsequent expressions. The coordinates (η, ξ) describe the proper time and position in the frame of a uniformly accelerating observer, with world-lines of constant ξ corresponding to hyperbolic trajectories in Minkowski spacetime.

The massless Klein-Gordon equation in Rindler coordinates is

$$\Box\phi = e^{-2a\xi}(-\partial_\eta^2 + \partial_\xi^2)\phi = 0 \tag{9}$$

The wave equation retains the same structure as the Minkowski case, up to the overall conformal factor $e^{-2a\xi}$. Since this factor does not affect the null structure of the equation, the mode solutions retain the same plane wave form but in the Rindler coordinates

$$r_k(\eta,\xi) = \frac{1}{\sqrt{4\pi\omega_k}}e^{-i(\omega_k\eta-k\xi)} + \text{h.c.} \tag{10}$$

for each wave number k and positive frequency $\omega_k = |k| > 0$. These "Rindler modes" are in terms of η and ξ and are thus confined to the Rindler wedge W. Since Rindler coordinates only cover W (the right wedge), these modes are not defined globally in Minkowski space.

---

[1] All diagrams follow the convention of t increasing upward and x increasing to the right.
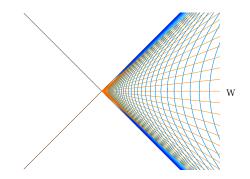
Figure 1: Rindler wedge W on the right.

2.2 Unruh Modes

To review how a uniformly accelerated observer perceives the Minkowski vacuum as a thermal bath, we construct the Unruh modes[1], analytic continuations of Rindler modes that are positive-frequency solutions with respect to Minkowski time[2]. From now on let $\omega_k = k > 0$.

We define constants α_k and β_k which satisfy $\alpha_k^2 - \beta_k^2 = 1$

$$
\begin{aligned}
\alpha_k &= \frac{e^{\frac{\pi \omega_k}{2a}}}{\sqrt{2 \sinh \frac{\pi \omega_k}{a}}} = \sqrt{\frac{1}{1 - e^{-2\pi \omega_k/a}}} \\
\beta_k &= \frac{e^{\frac{-\pi \omega_k}{2a}}}{\sqrt{2 \sinh \frac{\pi \omega_k}{a}}} = \sqrt{\frac{1}{e^{2\pi \omega_k/a} - 1}} \quad \text{(thermal form)}
\end{aligned}
\tag{11}
$$

They show up throughout in mode normalizations[3], inner products, and resulting Bogoliubov transforms. β_k also describes particle creation in terms of $|\beta_k|^2$ which has a thermal character, matching a Planck distribution at temperature $T = \frac{a}{2\pi}$.

Let $\widetilde{W}$ be the left Rindler wedge[4], $x < -|t|$ with Rindler modes $l_{\pm k}$. We analytically continue[5] the Rindler modes r_k, r_{-k}, l_k and l_{-k} into the (t, x) plane, these are the Unruh modes

$$
\begin{aligned}
\mu^R_{\pm k} &= \frac{\alpha_k}{\sqrt{4\pi\omega_k}}(a(\mp t + x \pm i\epsilon))^{\pm \frac{i\omega_k}{a}} & \mu^R_{\pm k|W} &\to \alpha_k r_{\pm k} \\
\mu^L_{\pm k} &= \frac{\alpha_k}{\sqrt{4\pi\omega_k}}(a(\mp t - x \pm i\epsilon))^{\pm \frac{i\omega_k}{a}} & \mu^L_{\pm k|\widetilde{W}} &\to \alpha_k l_{\pm k}
\end{aligned}
\tag{12}
$$

We added an $i\epsilon$ prescription to dictate which branch of the log to take so that the modes are analytic and bounded on the $\Im(t) < 0$ half plane. This makes the modes positive-frequency with respect to t. Another way of writing the Unruh modes is

$$
\begin{aligned}
\mu^R_{\pm k} &= \alpha_k r_{\pm k} + \beta_k l^*_{\mp k} \\
\mu^L_{\pm k} &= \alpha_k l_{\pm k} + \beta_k r^*_{\mp k}
\end{aligned}
\tag{13}
$$

where the right and left modes ($r_{\pm k}$ and $l_{\pm k}$) are understood to be zero outside of their respective wedges. See Figure 2 for an illustration of the Unruh modes. The magnitude shown jumps across the branch cut and conjugates the phase. Also, note that we have "twice as many" Unruh modes as we have Rindler modes; we double count each r_k with two analytic extensions μ^R_k and μ^{L*}_{-k}, and similarly for the left modes.

The Unruh modes form an alternative orthonormal basis of solutions to the Klein-Gordon equation, distinct from the plane waves $\varphi_{\pm k}$ see the original source Unruh[1].

---

[2] We mean that the modes contain no negative frequency Minkowski components.

[3] The normalizations come from computing the Klein Gordon inner product on Minkowski space and comparing it to inner products on W and $\widetilde{W}$.

[4] Coordinates on this wedge are $t = -\frac{1}{a}e^{a\delta}\sinh(a\gamma)$, $x = -\frac{1}{a}e^{a\delta}\cosh(a\gamma)$; and $l_{\pm k} = \frac{1}{\sqrt{4\pi\omega_k}}e^{i\omega_k(\gamma \pm \delta)}$.

[5] From the definitions and properties of sinh and cosh, it follows that $a(\pm t + x) = e^{a(\pm \eta + \xi)}$ and then $r_{\pm k} = e^{\pm \frac{i\omega_k}{a}\log a(\mp t + x \pm i\epsilon)}$. Similar statements hold for the left wedge.

The Unruh modes diagonalize (we will see in equation (17)) the Minkowski vacuum in terms of Rindler particle states and thus provide the natural framework for describing the Unruh effect and the thermal response perceived by uniformly accelerated observers.
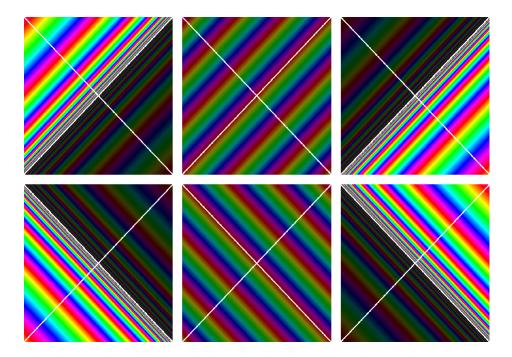

Figure 2: Spacetime diagrams of the $k > 0$ mode functions $\begin{bmatrix} \mu^L_{-k} & \varphi_k & \mu^R_k \\ \mu^L_k & \varphi_{-k} & \mu^R_{-k} \end{bmatrix}$. Color encodes the phase; brightness indicates magnitude. The Unruh modes change magnitude and conjugate phase across the log branch due to the interpretation of $\log(-1 \pm i\epsilon)$. The left-moving modes (top) correspond to emission in Minkowski space; the right-moving modes (bottom) to absorption.

2.3 Bogoliubov Transforms

We generalize the wedge W to a translated wedge W_c with apex $(0, c)$

$$W_c = \{(t, x) : x - c > |t|\} \tag{14}$$

and a reflected (left) wedge $\widetilde{W}_c$ with apex $(0, c)$

$$\widetilde{W}_c = \{(t, x) : x - c < -|t|\}. \tag{15}$$

Let the superscripts (0), (c), $(\widetilde{c})$, and (M) represent the W_0, W_c, $\widetilde{W}_c$, and Minkowski frames of reference respectively. Let $(A \to B)$ represent an open set inclusion[6] $A \subseteq B$.

This allows us to directly compute $W_0 \to M$ Bogoliubov coefficients from equation (13) for a change of basis from $a_q^{(M)}$ to c_q^R and c_q^L

$$\phi = \int dq \ \mu_q^R c_q^R + \mu_q^L c_q^L + \text{h.c.} \tag{16}$$

---

[6]In the algebraic formulation of QFT, spacetime regions correspond to operator algebras. Here, we adopt a complementary (though formally contravariant) perspective, whereby shifts in the wedge induce Bogoliubov transformations between operator algebras.

We find a 4 by 4 block matrix with blocks of the form

$$
\begin{bmatrix} a_k^{(0)} \\ a_{-k}^{\widetilde{(0)}\dagger} \end{bmatrix} = \begin{bmatrix} \alpha_k & \beta_k \\ \beta_k & \alpha_k \end{bmatrix} \begin{bmatrix} c_k^R \\ c_{-k}^{L\dagger} \end{bmatrix} \tag{17}
$$

and three others, where the $a_{-k}^{\widetilde{(0)}\dagger}$ is a left wedge creation operator. We can summarize the transform in the right wedge W as

$$
a_k^{(0)} = \alpha_k c_k^R + \beta_k c_{-k}^{L\dagger} \tag{18}
$$

and three other similar relations for $a_{-k}^{(0)}$, $a_k^{(0)\dagger}$, and $a_{-k}^{(0)\dagger}$.

We next compute the more general non-diagonal mixed Bogoliubov transformations.

$$
\begin{aligned}
(c \to M): \quad a_k^{(c)} &= \int \mathrm{d}q \; \alpha_{kq}^{(c \to M)} a_q^M + \beta_{kq}^{(c \to M)} a_q^{(M)\dagger} \\
(c \to 0): \quad a_k^{(c)} &= \int \mathrm{d}q \; \alpha_{kq}^{(c \to 0)} a_q^{(0)} + \beta_{kq}^{(c \to 0)} a_q^{(0)\dagger} \\
(\widetilde{c} \to 0): \quad a_k^{(\widetilde{c})} &= \int \mathrm{d}q \; \alpha_{kq}^{(\widetilde{c} \to 0)} a_q^{(0)} + \beta_{kq}^{(\widetilde{c} \to 0)} a_q^{(0)\dagger}
\end{aligned} \tag{19}
$$

We make use of a gamma function for $(c \to M)$. This occurs naturally in the KG dot product as an integral over an exponential phase from φ_k and a $(x - c)$ power from $r_k^{(c)}$ (the Mellin transform of e^{ikx} [5]):

$$
\begin{aligned}
\alpha_{kq}^{(c \to M)} &= \left\langle \varphi_q, r_k^{(c)} \right\rangle &= \frac{1}{2\pi a} \sqrt{\frac{\omega_k}{\omega_q}} \left(\frac{a}{q} \right)^{\frac{i\omega_k}{a}} e^{\frac{\pi \omega_k}{2a}} \Gamma\left(\frac{i\omega_k}{a} \right) \\
\beta_{kq}^{(c \to M)} &= \left\langle \varphi_q^*, r_k^{(c)} \right\rangle &= \frac{1}{2\pi a} \sqrt{\frac{\omega_k}{\omega_q}} \left(\frac{a}{q} \right)^{\frac{i\omega_k}{a}} e^{\frac{-\pi \omega_k}{2a}} \Gamma\left(\frac{i\omega_k}{a} \right)
\end{aligned} \tag{20}
$$

Next we consider products of shifted powers to go after $(c \to 0)$. We make use of a beta function for $(c \to 0)$ which occurs naturally in the KG dot product as an integral over a power of x and of $x - c$, from $r_k^{(0)}$ and $r_k^{(c)}$ respectively. We compute the Bogoliubov coefficients as

$$
\begin{aligned}
\alpha_{kq}^{(c \to 0)} &= \left\langle r_q^{(0)}, r_k^{(c)} \right\rangle = \frac{1}{2\pi a} \sqrt{\frac{\omega_k}{\omega_q}} (ac)^{\frac{i(\omega_k - \omega_q)}{a}} B\left(\frac{i\omega_k}{a}, \frac{-i(\omega_k - \omega_q)}{a} \right) \\
\beta_{kq}^{(c \to 0)} &= \left\langle r_q^{(0)*}, r_k^{(c)} \right\rangle = \frac{1}{2\pi a} \sqrt{\frac{\omega_k}{\omega_q}} (ac)^{\frac{i(\omega_k + \omega_q)}{a}} B\left(\frac{i\omega_k}{a}, \frac{-i(\omega_k + \omega_q)}{a} \right)
\end{aligned} \tag{21}
$$

The reflected diamond wedge version also yields a beta function, but with a different form

$$
\begin{aligned}
\alpha_{kq}^{(\widetilde{c} \to 0)} &= \left\langle r_q^{(0)*}, r_k^{(\widetilde{c})} \right\rangle = \frac{1}{2\pi a} \frac{\sqrt{\omega_k \omega_q}}{\omega_q - \omega_k} (ac)^{\frac{i(\omega_k - \omega_q)}{a}} B\left(\frac{i\omega_k}{a}, -\frac{i\omega_q}{a} \right) \\
\beta_{kq}^{(\widetilde{c} \to 0)} &= \left\langle r_q^{(0)}, r_k^{(\widetilde{c})} \right\rangle = \frac{1}{2\pi a} \frac{\sqrt{\omega_k \omega_q}}{\omega_q + \omega_k} (ac)^{\frac{i(\omega_k + \omega_q)}{a}} B\left(\frac{i\omega_k}{a}, \frac{i\omega_q}{a} \right)
\end{aligned} \tag{22}
$$

2.4 Modular Automorphisms

We can compare absolute magnitudes for M v.s. W_c and see that they don't depend on c

$$
\begin{aligned}
\left| \alpha_{kq}^{(c_1 \to M)} \right|^2 &= \left| \alpha_{kq}^{(c_2 \to M)} \right|^2 \\
\left| \beta_{kq}^{(c_1 \to M)} \right|^2 &= \left| \beta_{kq}^{(c_2 \to M)} \right|^2
\end{aligned} \tag{23}
$$

The c independence is expected in this case since Unruh radiation is translation invariant. We next turn to $(c \to 0)$ and also find c independence there

$$
\begin{aligned}
\left| \alpha_{kq}^{(c_1 \to 0)} \right| &= \left| \alpha_{kq}^{(c_2 \to 0)} \right| \\
\left| \beta_{kq}^{(c_1 \to 0)} \right| &= \left| \beta_{kq}^{(c_2 \to 0)} \right|
\end{aligned} \tag{24}
$$

This invariance is more surprising than in the Minkowski case, as it implies that the expected number of excitations for a mode $r_k^{(c_2)}$ when expressed in the vacuum of W_{c_1},

$$\int \mathrm{d}q \ |\beta_{kq}^{(c_2 \to c_1)}|^2 \tag{25}$$

is invariant[7] under changes in both c_1 and c_2.

More explicitly using the form of the c term in equations (21) and (22) we have a transform matrix of Λ_c from W_0 to W_c

$$\begin{bmatrix} a_k^{(c)} \\ a_{-k}^{(c)} \\ \hline a_k^{(c)\dagger} \\ a_{-k}^{(c)\dagger} \end{bmatrix} = \underbrace{\left[\begin{array}{cc|cc} A_c & 0 & B_c & 0 \\ 0 & -A_c & 0 & -B_c \\ \hline \overline{B_c} & 0 & \overline{A_c} & 0 \\ 0 & -\overline{B_c} & 0 & -\overline{A_c} \end{array} \right]_{k,q}}_{\Lambda_c} \begin{bmatrix} a_q^{(0)} \\ a_{-q}^{(0)} \\ \hline a_q^{(0)\dagger} \\ a_{-q}^{(0)\dagger} \end{bmatrix} \tag{26}$$

where $A_c = \alpha_{kq}^{(c \to 0)} = P_c A_1 P_c^{-1}$ and $B_c = \beta_{kq}^{(c \to 0)} = P_c B_1 P_c$ for a diagonal phase factor matrix

$$P_{c,rs} = \delta(r - s) c^{\frac{i\omega_r}{a}} = e^{\frac{iH}{a} \log c} \tag{27}$$

where H is the Rindler Hamiltonian associated with mode frequency ω_k. We can write Λ_c out compactly out as

$$\Lambda_c = Q_c \Lambda_1 Q_c^{-1} \tag{28}$$

where

$$Q_c = \begin{bmatrix} P_c, & 0 & 0 & 0 \\ 0 & P_c & 0 & 0 \\ 0 & 0 & P_c^{-1} & 0 \\ 0 & 0 & 0 & P_c^{-1} \end{bmatrix} \tag{29}$$

The composition of Bogoliubov transforms, $\Lambda_{nc} = \Lambda_c^n$, yields

$$\begin{aligned} Q_{nc}\Lambda_1 Q_{nc}^{-1} &= \Lambda_{nc} \\ &= (Q_c \Lambda_c Q_c)\left(Q_c^{-1}\Lambda_c Q_c\right) \cdots (Q_c \Lambda_c Q_c) \\ &= Q_c \Lambda_c^n Q_c^{-1} \end{aligned} \tag{30}$$

so that

$$\begin{aligned} \Lambda_c^n &= Q_c^{-1} Q_{nc} \Lambda_1 Q_{nc}^{-1} Q_c \\ &= Q_n \Lambda_1 Q_n^{-1} \end{aligned} \tag{31}$$

and more generally we have a one parameter unitary group under the modular parameter $x = \log c$, with generator H/a given by

$$\left\{ \Lambda_1^x = Q_x \Lambda_1 Q_x^{-1} : x \in \mathbb{R} \right\}. \tag{32}$$

So these Bogoliubov transformations between shifted wedges form a one-parameter group under translations of the apex, exhibiting a symmetry that parallels modular automorphism flow in algebraic QFT [6]. In contrast to traditional treatments emphasizing Lorentz boosts within a fixed wedge, this formulation reveals modular structure via spatial translations.

Consider a sequence

$$W_{c_n} \subseteq \cdots \subseteq W_{c_i} \subseteq \cdots \subseteq W_{c_j} \subseteq W_{c_2} \subseteq W_{c_1} \tag{33}$$

The result is that each inclusion $W_{c_i} \subseteq W_{c_j}$ yields the same "amount" and "type" of particle production, with fixed squared Bogoliubov magnitude $|\beta_{kq}|^2$, implying that the expected number of particles remains constant across all nested wedge pairs, independent of the actual values of c_i or c_j.

---

[7]Similar statements are true for reflected (diamond) wedges.

3 Driving Sources

We now turn to a foundational question: **"What, physically, is accelerating the observer?"** In standard Unruh-effect derivations, the acceleration is treated as given; here we supply a concrete, physical mechanism in the form of a localized, entangled source.

Acceleration has been introduced as a geometric feature, a coordinate choice, without reference to any underlying dynamical mechanism. Moreover, we have left unspecified both the observer's precise location within the Rindler wedge and the spatial origin of the detected excitations. These omissions reflect an effective coarse-graining over the details of the observer and their interaction with the field, a feature that contributes to the apparent thermality observed in the Unruh effect.
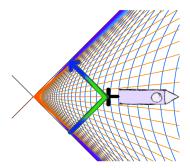

Figure 3: A Rindler mode's frequency is smeared out in Minkowski space, blue-shifted near the horizon. We diagram a particle as if it were striking a mirror at the rear of a rocket, where its reflection emerges as a combination of emission and absorption processes in the Rindler frame.

A natural physical interpretation is that a *driving source* must exist, both as the cause of the observer's acceleration, and as a localized field source coupled to the quantum field. In this view, acceleration is not merely a kinematic artifact or coordinate reparameterization, but the result of active, localized interactions along the observer's worldline. These interactions are responsible for the observer's motion. This plays well with the notion that the observer is not in an isotropic background radiation, but is actually thrusted away from the event horizon, the thrust being intimately correlated with the causal horizon.

Figure 3 illustrates the situation with a particle composed of Rindler modes on the right wedge. The modes r_k are left-moving, propagating toward the future horizon and associated with **emission**; the r_{-k} modes are right-moving, originating from the past horizon and are associated with **absorption**. These Rindler modes are constructed as superpositions of restricted Minkowski modes $\varphi_{q_{|W}}$, effectively smeared across a range of frequencies. This frequency mixing is evident in Figure 2, where the modes blue-shift infinitely near the horizons and red-shift infinitely at spatial infinity, due to the geometry of the wedge.

3.1 Construction

We motivate a construction of a driving source using an example pictured in Figure 4. The observer on the right at $(t, x) = (0, 1)$ is named Wright and we also have an observer on the left at $(0, -1)$ named Lester. A common causal ancestor exists in the past, Paz at $(-1, 0)$. Paz emits an entangled pair of photons with (Rindler) frequency $\omega = \omega_{\pm k}$ as part of a stream of photons that are the source, and cause, of the acceleration of Wright and of Lester. The accelerations are thus correlated.

Now where we usually would create a localized detector for Wright, such as an Unruh-DeWitt detector [1] [7] interacting with the field, we instead seek to model the situation
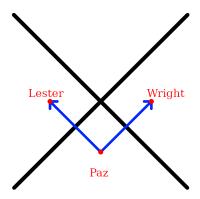
Figure 4: A thruster in the past, Paz, emits an entangled photon pair that accelerates Wright (to the right) and Lester (to the left).

where Paz, a *thruster*, is coupled to the field. This inversion of effect and cause, of detector and thruster, is at the heart of our construction. Paz's emission makes the source of the acceleration manifest as particle injection, so that Wright will make sense of a *guaranteed* observation of a "thrust particle" with fixed peaked momentum ω_{-k}. Wright's detection is entangled with Lester's, so Lester will also observe a particle with momentum ω_k, measurement induced correlation.

Physically, Paz introduces a bilocal source J

$$J(x,y) = \lambda f_L(x) f_R(y)$$
$$\mathcal{L}_{sourced} = \mathcal{L}_{free} + J\phi \tag{34}$$

This source construction is standard to QFT [2] [8] as a coupling of a classical function with the field as an interaction term $J\phi$. In this version J acts coherently on the field shifting the modes in both wedges simultaneously, creating correlations that build entanglement at the level of a global quantum state. The product structure reflects this paired excitation, with f_L and f_R defining the mode profiles localized respectively in the left and right Rindler wedges. This is a paired global-coherent version of the usual vacuum squeezing.

To analyze a mode f_R in the right wedge, we pair the mode with a complementary mode in the left wedge f_L. This setup is compatible with the standard thermal vacuum description[8] of the Unruh effect

$$|0\rangle_M = \prod_\omega \frac{1}{\cosh\theta_k} \sum_n \tanh^n \theta_k \, |n_\omega\rangle_L \, |n_\omega\rangle_R. \tag{35}$$

This state factorizes into correlated excitations in the left (L) and right (R) wedges. The Unruh mode associated with frequency ω is a specific linear combination of L and R Rindler modes, so that any source J coupling to it will, in general, drive correlated excitations across both wedges. For example, the state prepared by Paz corresponds to a selective $n = 1$ excitation at a fixed ω,

$$|\Psi_\omega\rangle = |1_\omega\rangle_L \, |1_\omega\rangle_R + \mathrm{O}(\text{higher terms}), \tag{36}$$

a controlled approximation of one term in the ensemble. Our source singles out the $n_\omega = 1$ term, giving a selected "slice" of the full thermal ensemble. The source $J(x,y)$ does not contradict the thermal interpretation, but rather describes a specific "microstate" consistent with the broader thermal ensemble.

An illustration of this setup is shown in Figure 5. From this perspective, the apparent thermality arises from intrinsic properties of the vacuum, an effective ignorance of the source's detailed structure and dynamics. In this view, the Unruh effect is not a passive revelation of hidden particles in the vacuum, but a measurable consequence of *thrust*.

---

[8] The form of this vacuum equation can be proven by recursively applying the Bogoliubov relations in equation (18). θ_k is chosen to match $\alpha_k = \cosh\theta_k$ and $\beta_k = \sinh\theta_k$ from equation (11) so $\tanh\theta_k = \frac{\beta_k}{\alpha_k} = e^{-\pi\omega_k/a}$.
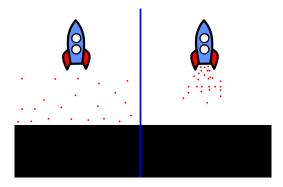
Figure 5: Conceptual illustration of thermal v.s. localized acceleration.

3.2 Physical Details

The construction of the absorption function f_R for Wright presents some physical challenges. The first is that the actual coherent state obtained from J contains terms at higher particle numbers. We either assume strongly that the state is exactly prepared, or that $\tanh \theta_k$ is sufficiently small as to make the higher terms negligible.

The second challenge is that we are integrating over the entire Minkowski space instead of over a short time period as normally desired for a source J. This challenge is met by noticing that our integral of eternal modes f_R (and f_L) can be replaced by an integral over a small time interval $|t + 1| < \delta$ around Paz's time $t = -1$. These two integrals are seen to be proportional using Stokes' theorem, see Figure 6 (right picture). It is also manifestly evident that the integrals are proportional by the fact that the mode is translation invariant over time and space, $f_R(t, x) = f_R(-1, x + t + 1)$, since it is a sum of right moving Minkowski modes. The coupling constant λ in equation (34), along with δ, can be chosen to match the vacuum equation (35) at $n_\omega = 1$.
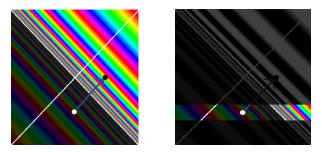

Figure 6: The points marked with black and white dots at (0,1) (Wright) and (-1,0) (Paz) respectively in the left picture lie on the same Unruh mode trajectory; although the mode is infinitely blue-shifted at the horizon, the total Doppler effect between these two locations cancels, so the mode represents the same local frequency ω. The right figure illustrates a finite time interval of width δ for the source J to be active.

Another detail is that J is described in the Rindler basis, so Paz will need to couple to an Unruh mode – the analytically continued Rindler mode (see Section 2). This mode undergoes an infinite blue shift at the horizon, but is more well behaved at Wright and Paz's locations. In subsequent sections, we aim to localize f_R away from the high-frequency, near-horizon behavior typical of thermal modes, making the physical realization of the source J more plausible as a localized wave packet.

Finally, we emphasize that our running example represents just one of many possible mechanisms for exchanging energy and correlations between wedges.

For the remainder of this note, we focus on the modes f_R in the right wedge without explicit reference to f_L, operating under the assumption that the localized driving source in the right wedge arises from a globally entangled paired source.

3.3   Back in Time Story

An interesting side note is that Lester's proper time (Rindler time) in the left wedge is flowing in reverse to Minkowski time. So we can actually track the story[9] as:

1. Lester emits a particle traveling back in time.

2. Paz receives this particle and reflects it forward in time to Wright.

3. Wright then absorbs the particle.

The presence of virtual particle-antiparticle pairs in massive scalar fields further enriches this picture, where antiparticles are understood as particles moving "back in time", though this extension lies beyond the scope of this present note.

3.4   Sub-Wedge Causal Chain

The sub-wedge sequence mentioned in equation (33) has an interesting interpretation. The vacuums are entangled from each wedge to the next sub-wedge. In our in construction, this is understood as a causal chain from Paz to Wright. Each sub-wedge inherits a source J from the previous.

4   Localization

4.1   Localization via Translated Wedge Inclusion

Consider the two nested Rindler wedges $W_c \subseteq W_0$ shown in Figure 7. Let r_q denote a Rindler mode[10] associated with W_0, analytically continued to the entire Minkowski space. The gray-scale region indicates the full support of r_q, while the rainbow-colored segment shows its restriction to the sub-wedge W_c.

By considering the restriction of r_q to W_c, we have partially localized the observer and the mode. The restriction effectively cuts off the high-frequency content of r_q near the future horizon[11] of W_0. The resulting mode still spans the full spatial extent of W_c, but it is now insulated from the highly oscillatory behavior near the horizons of W_0. The localization is not complete however, the observer can still be anywhere within the wedge W_c, and the corresponding modes r_k still exhibit thermal characteristics because of low-frequency oscillations extending throughout the wedge.

To further study the situation, consider the modulus squared inner product $\left| \left\langle r_q^{(0)}, r_k^{(c)} \right\rangle \right|^2$, also known as the Bogoliubov $\left| \alpha_{kq}^{(c \to 0)} \right|^2$, from equation (21). We fix q and use $|\Gamma(ib)|^2 = \frac{\pi}{b \sinh \pi b}$ to obtain

$$\left| \left\langle r_q^{(0)}, r_k^{(c)} \right\rangle \right|^2 = \frac{\sinh \frac{\pi \omega_q}{a}}{4\pi a (\omega_q - \omega_k) \sinh \pi \frac{\omega_q - \omega_k}{a} \sinh \frac{\pi \omega_k}{a}} \tag{37}$$

as a function of ω_k. The function exhibits a second-order pole at $\omega_k = \omega_q$, resulting in a sharply peaked feature, see Figure 8. Although the sinh terms encode aspects of the

---

[9]We can interchange these emission and absorption stories, Wright emits and Lester absorbs, but we would need to involve an observer in the future at $(t, x) = (1, 0)$ for that.

[10]From here on we often interchange Rindler and Unruh modes since we are only concerned with the restriction to the right wedge or subsets.

[11]Similarly, r_{-q} experiences suppression near the past horizon.
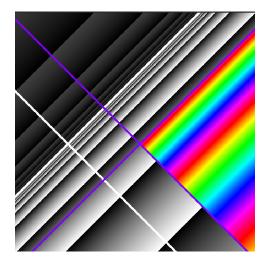
Figure 7: A Wedge W_c (blue) inside of the wedge W_0 (white). Rindler mode r_q of W_0 (gray-scale) restricted to W_c (rainbow).

familiar thermal distribution, especially broadening near $\omega_k = 0$, the existence of the peak itself at $\omega_k = \omega_q$ originates from the geometric restriction, not from a detector's passive response to the vacuum, but as the active spectral footprint of a localized source.
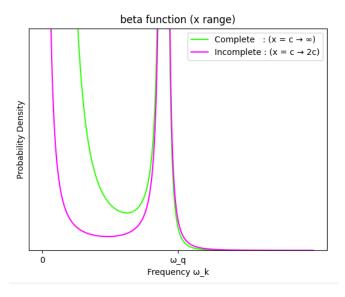

Figure 8: The Rindler modes r_k of W_c show a peaked spectral overlap with r_q at $\omega_k = \omega_q$. The incomplete beta function picks out the spectral peak suppressing the peak at zero.

4.2 Diamond Localization via Reflected Wedge Intersection

Further localization is achieved by intersecting W_c with a reflected wedge $\widetilde{W}_{2c}$. This defines a more tightly localized diamond-shaped region, as shown in Figure 9. The mode r_q is now restricted to the intersection $W_c \cap \widetilde{W}_{2c}$, which eliminates much of the infrared behavior previously associated with the unrestricted wedge.

The Klein Gordon inner product at $t = 0$ now takes the form of an incomplete version

of the beta function from equation (21), corresponding to an integral[12] evaluated from c to $2c$ rather than extending to infinity. This inner product does not however correspond to a mode expansion of the field, since the analytic continuation of the diamond would be to all of W_c, or all of $\widetilde{W}_{2c}$, in which case the mode would no longer be localized to the diamond. So it is no longer invariant to integrate along a Cauchy surface for the inner product; this construction does not define a complete orthonormal set, and cannot be used to build a full basis of field modes.

This motivates a shift in perspective: rather than interpreting r_q as part of a global mode expansion, we regard it as a compactly supported, non-invariant test function, i.e., a driving source localized to the diamond region, consistent with the source framework introduced in Section 3. We turn on r_q exactly for a fixed period of $x-t$ (or $x+t$ for r_{-q}). The resulting spectral response in the diamond, computed from this truncated integral, is shown[13] in Figure 8.

The plot reveals that the main spectral peak at $\omega_k = \omega_q$ persists, while the thermal contribution near $\omega = 0$ is significantly attenuated.
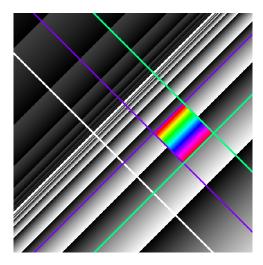

Figure 9: The same situation as in Figure 7 but we further intersect with a reflected (left) wedge $\widetilde{W}_{2c}$ (green). Rindler mode r_q of W_0 (gray-scale) restricted to $W_c \cap \widetilde{W}_{2c}$ (rainbow).

4.3 Thermal to Localized Interpolation

To further probe how global thermal structure transitions into a localized excitation profile, we consider the behavior of Rindler-to-Minkowski Bogoliubov coefficients when weighted by a Gaussian envelope. This allows us to interpolate between de-localized (thermal) and localized (spectrally peaked) behavior. We use parabolic cylinder functions [9, 10] which are the analytic continuation of

$$D_\nu(-z) = \frac{e^{-\frac{1}{4}z^2}}{\Gamma(-\nu)} \int_0^\infty \mathrm{d}s\ e^{zs} s^{-\nu-1} e^{-\frac{1}{2}s^2}, \Re\nu < 0, \tag{38}$$

where we use $-z$ instead of the usual z so that future equations become simpler.

Without loss of generality, let $N_{\mu,\sigma} = e^{-\frac{1}{2}\frac{(x-t-\mu)^2}{\sigma^2}}$ be a (left-moving) Gaussian kernel with fixed μ. We will multiply φ_q^* by $N_{\mu,\sigma}$, but we could just as easily multiply r_k by $N_{\mu,\sigma}$

---

[12]We could also use the other form of the beta function in equation (22) to compute the same inner product.

[13]The green (complete) beta function curve is actually independent of the choice of translation c, it is the same curve for any sub-wedge space-like inclusion (see Modular Automorphism Section 2.4). In contrast, the incomplete beta function curve (magenta) does depend on the endpoint ($2c$ is shown).

for the same effect. A key aspect of this construction is that the resulting Minkowski modes are treated as driving sources rather than elements of an orthonormal mode expansion. Since we are not working within an orthonormal mode expansion, the normalization of $N_{\mu,\sigma}$ is left implicit. For clarity, since this setup may be non-standard, we carry out the calculations explicitly in this section. We will examine the $N_{\mu,\sigma}$ modification of $\beta_{kq}^{(c\to M)}$ in equation (20)

$$
\begin{aligned}
\left\langle \varphi_q^* N_{\mu,\sigma}, r_k \right\rangle &= \frac{1}{4\pi\sqrt{\omega_q\omega_k}} 2i \int_{\Sigma_W} e^{-i(\omega_q t - qx)} e^{-\frac{1}{2}\frac{(x-t-\mu)^2}{\sigma^2}} \partial_t (a(x-t))^{\frac{i\omega_k}{a}} \\
&= \frac{1}{2\pi}\sqrt{\frac{\omega_k}{\omega_q}} a^{\frac{i\omega_k}{a}-1} \int_0^\infty \mathrm{d}x \, e^{-\frac{1}{2}\frac{(x-\mu)^2}{\sigma^2}+iqx} x^{\frac{i\omega_k}{a}-1} \\
&= \frac{1}{2\pi}\sqrt{\frac{\omega_k}{\omega_q}} a^{\frac{i\omega_k}{a}-1} \int_0^\infty \mathrm{d}x \, e^{\left(-\frac{1}{2\sigma^2}\right)x^2 + \left(\frac{\mu}{\sigma^2}+iq\right)x + \left(-\frac{\mu^2}{2\sigma^2}\right)} x^{\frac{i\omega_k}{a}-1} \\
&= \frac{1}{2\pi a}\sqrt{\frac{\omega_k}{\omega_q}} e^{-\frac{\mu^2}{2\sigma^2}} \sigma^{\frac{i\omega_k}{a}} a^{\frac{i\omega_k}{a}} \int_0^\infty \mathrm{d}s \, e^{\left(\frac{\mu}{\sigma}+iq\sigma\right)s} s^{\frac{i\omega_k}{a}-1} e^{-\frac{1}{2}s^2} \\
&= \frac{1}{2\pi a}\sqrt{\frac{\omega_k}{\omega_q}} e^{-\frac{\mu^2}{2\sigma^2}} (\sigma a)^{\frac{i\omega_k}{a}} e^{\frac{1}{4}\left(iq\sigma+\frac{\mu}{\sigma}\right)^2} \Gamma\left(\frac{i\omega_k}{a}\right) D_{-\frac{i\omega_k}{a}}\left(-iq\sigma-\frac{\mu}{\sigma}\right) \\
&= \frac{1}{2\pi a}\sqrt{\frac{\omega_k}{\omega_q}} e^{-\frac{\mu^2}{2\sigma^2}} (\sigma a)^{\frac{i\omega_k}{a}} e^{\frac{1}{4}z^2} \Gamma(-\nu) D_\nu(-z)
\end{aligned}
\tag{39}
$$

where Σ_W is the Cauchy surface $\eta = 0$ on the Rindler wedge W, $x = \sigma s$, $z = iq\sigma + \frac{\mu}{\sigma}$, and $\nu = -\frac{i\omega_k}{a}$. And then

$$
\left| \left\langle \varphi_q^* N_{\mu,\sigma}, r_k \right\rangle \right|^2 = \frac{1}{2\pi a\omega_q} \frac{\omega_k}{2\pi a} e^{-\frac{\mu^2}{\sigma^2}} \left| e^{\frac{1}{2}z^2} \right| |\Gamma(-\nu)|^2 |D_\nu(-z)|^2
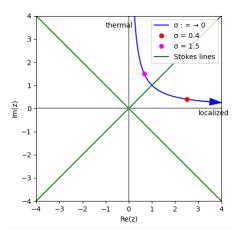\tag{40}
$$

From [10] we have

Figure 10: Trajectory of $z = iq\sigma + \frac{\mu}{\sigma}$ as σ interpolates between thermal and localized regimes. For σ starting at ∞, the trajectory starts at the positive infinite imaginary axis, aligning with the dominant thermal component of the excitation. As $\sigma \to 0$, the system crosses a Stokes line and transitions into a sharply localized, source-driven configuration, where thermal character disappears. See also corresponding Figure 11.

$$
D_\nu(-z) = e^{-i\pi\nu} z^\nu e^{-\frac{1}{4}z^2} \{1 + O(|z|^{-2})\} + \frac{(2\pi)^{\frac{1}{2}}}{\Gamma(-\nu)} z^{-\nu-1} e^{\frac{1}{4}z^2} \{1 + O(|z|^{-2})\}
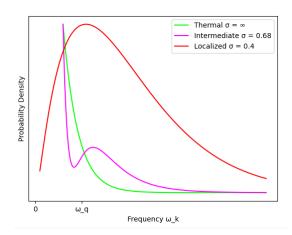\tag{41}
$$

Figure 11: $\left|\left\langle \varphi_q^* N, r_k \right\rangle\right|^2$ for various values of σ (probability density is scaled for comparison). $\omega_q = 1$, $q = 1$, $a = 1$, $\mu = 1$. See also corresponding Figure 10.

when $-\frac{1}{4}\pi + \epsilon \leq \arg z \leq \frac{3}{4}\pi - \epsilon$.

The two asymptotic regimes correspond to physically distinct interpretations: The second $e^{\frac{1}{4}z^2}$ term dominates for $z \to \infty$ as $\sigma \to 0$ and the first $e^{-\frac{1}{4}z^2}$ term dominates for $z \to i\infty$ as $\sigma \to \infty$. This is a Stokes phenomenon[14] which flips over as we cross the Stokes line at $\arg z = \frac{\pi}{4}$. The situation is pictured in Figure 10.

We next combine equations (40) and (41). First for the thermal part that comes from the $e^{-\frac{1}{4}z^2}$ term where $\sigma \to \infty$ we have

$$
\begin{aligned}
2\pi a \omega_q \left|\left\langle \varphi_q^* N, r_k \right\rangle\right|^2 &= \frac{\omega_k}{2\pi a} e^{-\frac{\mu^2}{\sigma^2}} \left| e^{-i\pi\nu} z^\nu \Gamma\left(\frac{i\omega_k}{a}\right)\right|^2 \\
&= \frac{\omega_k}{2\pi a} e^{-\frac{\mu^2}{\sigma^2}} e^{\frac{-2\pi\omega_k}{a}} \left| e^{\frac{-2i\omega_k}{a} \log\left(\frac{\mu}{\sigma}+iq\sigma\right)}\right|^2 \frac{\pi}{\frac{\omega_k}{a} \sinh \frac{\pi\omega_k}{a}} \\
&\to e^{\frac{-2\pi\omega_k}{a}} \left| e^{\frac{-2i\omega_k}{a} \log i}\right|^2 \frac{1}{2 \sinh \frac{\pi\omega_k}{a}} \\
&= e^{\frac{-2\pi\omega_k}{a}} e^{\frac{\pi\omega_k}{a}} \frac{1}{\left(e^{\frac{\pi\omega_k}{a}} - e^{\frac{-\pi\omega_k}{a}}\right)} \\
&= \frac{1}{e^{\frac{2\pi\omega_k}{a}} - 1}
\end{aligned}
\tag{42}
$$

which we expect by construction. For the localized part that comes from the $e^{\frac{1}{4}z^2}$ term where $\sigma \to 0$ we have

$$
\begin{aligned}
2\pi a \omega_q \left|\left\langle \varphi_q^* N, r_k \right\rangle\right|^2 &= \frac{\omega_k}{a} e^{-\frac{\mu^2}{\sigma^2}} \left| e^{z^2} z^{2(-\nu-1)}\right| \\
&= \frac{\omega_k}{a} e^{-\frac{\mu^2}{\sigma^2}} \left| e^{\left(iq\sigma+\frac{\mu}{\sigma}\right)^2} e^{2\left(\frac{i\omega_k}{a}-1\right) \log\left(iq\sigma+\frac{\mu}{\sigma}\right)}\right| \\
&\to \frac{\omega_k}{a} e^{\frac{-2\epsilon\omega_k}{a}} f(\sigma, \mu)
\end{aligned}
\tag{43}
$$

where the thermal pole at zero has disappeared. While the precise asymptotic form is not critical, we can control the ultraviolet behavior by taking z to $(1+i\epsilon)\infty$ which remains within in the localized Stokes region. This introduces a regulating factor of the form $e^{-2\epsilon\omega_k/a}$, which suppresses high-frequency contributions.

---

[14]See [11] for a similar approach where the Stokes phenomenon is applied to particle production in simple expanding backgrounds, preheating after R^2 inflation, and a transition model with smoothly changing mass.

We should stop short of σ actually reaching zero, since that is a localization to an extreme, where $N_{\mu,\sigma}$ shrinks to a bump with infinitesimal width; This is not a delta function, it is a vanishing source. We focus on the small-but-nonzero σ regime where the thermal character has already disappeared. See Figure 11 for representative plots across varying values of σ.

5   Conclusion

This work examined the Unruh phenomenon from a localized perspective, emphasizing its manifestation as a physically driven effect rather than a purely thermal one. By restricting Rindler modes to translated and reflected wedges, and their intersections, we showed that the apparent thermal behavior can be partially eliminated. As these modes become localized, the traditional detector response, typically interpreted as a thermal signature of entanglement across a causal horizon, is here reinterpreted as the spectral imprint of a localized, dynamically sourced excitation. We then showed that the mixed Bogoliubov inner product between Minkowski and Rindler modes provides a smooth interpolation from global thermality to a localized spectral structure, with parabolic cylinder functions encoding this transition in analytic form.

Our approach complements the traditional detector-based interpretation by highlighting the role of the physical agent causing acceleration as an active source of field excitations. This perspective does not contradict the well-known thermality arising from entanglement but offers a localized, dynamical viewpoint that may better capture realistic scenarios.
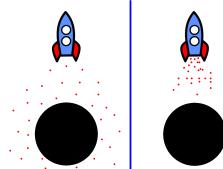

Figure 12:   Conceptual illustration contrasting global Hawking radiation (left) with a localized, source-driven excitation near a black hole (right). Compare with Figure 5.

While our analysis is grounded in flat spacetime, the equivalence principle offers a natural pathway for extending this framework to curved geometries. In particular, future work could explore applications to Hawking radiation by modeling localized excitations near black hole horizons. Figure 12 offers a schematic illustration of this idea, emphasizing a shift from thermal emission to localized, physically sourced excitations in the near-horizon region.

Finally, if the ideas presented here are correct, the thermal signature observed in the Unruh effect can always be traced back to a causal source. Experimentally, this implies that Unruh radiation should not appear isotropic, and randomly, but should be associated with specific, identifiable, accelerating "thrust particles". Conversely, the absence of a thermal Unruh signal in scenarios where a known accelerating source exists would provide experimental evidence supporting this framework. The construction of such an experiment is made difficult by the intrinsic weakness of the Unruh effect.

6 Acknowledgments

References

[1] W. G. Unruh, "Notes on black-hole evaporation," *Physical Review D*, vol. 14, no. 4, p. 870, 1976.

[2] J. Schwinger, "Particles and sources," *Physical Review*, vol. 152, p. 1219â€"1226, Dec. 1966.

[3] E. Frodden and N. Valdes, "Unruh effect: Introductory notes to quantum effects for accelerated observers," *International Journal of Modern Physics A*, vol. 33, no. 27, p. 1830026, 2018.

[4] W. Rindler, "Kruskal space and the uniformly accelerated frame," *Am. J. Phys*, vol. 34, no. 12, pp. 1174–1178, 1966.

[5] R. Bracewell and P. B. Kahn, "The fourier transform and its applications," *American Journal of Physics*, vol. 34, no. 8, pp. 712–712, 1966.

[6] H. J. Borchers, "On revolutionizing quantum field theory with tomita's modular theory," *Journal of mathematical Physics*, vol. 41, no. 6, pp. 3604–3673, 2000.

[7] A. Einstein, *General Relativity: An Einstein Centenary Survey*. Cambridge University Press, 1979.

[8] L. H. Ryder, *Quantum field theory*. Cambridge university press, 1996.

[9] M. Abramowitz and I. A. Stegun, eds., *Handbook of Mathematical Functions with Formulas, Graphs, and Mathematical Tables*, vol. 55 of *Applied Mathematics Series*. Washington, D.C.: U.S. Government Printing Office, 1964. Reprinted 1983. See Chapter 19.

[10] F. W. J. Olver, "Uniform asymptotic expansions for weber parabolic cylinder functions of large orders," *Journal of Research of the National Bureau of Standards. Section B, Mathematical Sciences*, vol. 63B, pp. 131–169, 1959.

[11] S. Hashiba and Y. Yamada, "Stokes phenomenon and gravitational particle production—how to evaluate it in practice," *Journal of Cosmology and Astroparticle Physics*, vol. 2021, no. 05, p. 022, 2021.

[12] N. Beisert, "Quantum field theory i," *ETH Zurich, HS12*, 2012.